Cell-Cell Fusion in NSCLC Confers a Fitness Benefit Under Drug Selection

Paulameena V. Shultes[1, 2, +], Dagim S. Tadele[2, 3, +], Arda Durmaz[2], Davis T. Weaver[2], Rowan Barker-Clarke[2], Mina N. Dinh[2], Siqing Liu[4], Endalkachew A. Alemu[4], Simon Rayner[4], and Jacob G. Scott[2, *]

[1]Case Western Reserve University, School of Medicine, Cleveland, OH, USA
[2]Cleveland Clinic Foundation, Translational Hematology and Oncology Research Division, Cleveland, OH, USA
[3]Oslo University Hospital, Department of Medical Genetics, Oslo, Norway
[4]Department of Medical Genetics, Oslo University Hospital, University of Oslo, 0450 Oslo, Norway
[*]scottj10@ccf.org
[+]these authors contributed equally to this work

ABSTRACT

Cell-cell fusion has been implicated in various physiological and pathological processes, including cancer progression. This study investigated the role of cell-cell fusion in non-small cell lung cancer (NSCLC), focusing on its contribution to chemoresistance and tumor evolution. By co-culturing drug-sensitive and drug-resistant NSCLC cell lines, we observed spontaneous cell-cell fusion events, particularly under gefitinib selection. These fused cells exhibited enhanced fitness and a higher degree of chemoresistance compared to parental lines across a panel of 12 chemotherapeutic agents. Further analysis, including fluorescence imaging and cell cycle analysis, confirmed nuclear fusion and increased DNA content in the fused cells. Bulk RNA sequencing revealed genomic heterogeneity in fused cells, including enrichment of gene sets associated with cell cycle progression and epithelial-mesenchymal transition, hallmarks of cancer malignancy. These findings demonstrate that cell-cell fusion contributes significantly to therapeutic resistance and the promotion of aggressive phenotypes in NSCLC, highlighting its potential as a therapeutic target.

Introduction

Cell-cell fusion is a complex process characterized by cellular approach, adhesion, membrane pore opening, cytoplasmic mixing, and in some cases nuclear mixing.[1] Despite this complexity, spontaneous cell-cell fusion occurs throughout the human body and appears to characterize different aspects of human physiology and pathology.[2] Current literature suggests that in humans, the roles of cell-cell fusion vary from embryogenesis and placentation to increasing cancer malignant potential .[2–4] There is increasing evidence of the potential for cell-cell fusion to potentiate cancer malignancy, yet in general, the process of cell-cell fusion has not been studied extensively in many cancers, including non-small cell lung cancer (NSCLC).[2,4]

Non-small cell lung cancer accounts for the majority ($\tilde{8}5\%$) of lung cancers, and is one of the leading causes of cancer-related deaths worldwide.[5] Genomic characterization has identified common oncogenes such as EGFR that serve as molecular targets for modern NSCLC chemotherapeutics.[5] Current treatments for NSCLC vary in efficacy, and like many cancers, NSCLC patients can and often do evolve chemoresistance to the standard immunologic and chemotherapeutics through a variety of mechanisms, including immune evasion.[5,6] A recent study identified that cell-cell fusion directly contributes to NSCLC immune evasion and decreased efficacy of PD-L1 immunologic agents.[7] This raises the question of how else cell-cell fusion can contribute to the increased rates of treatment failure in NSCLC patients.

In this study, we have isolated and characterized NSCLC (PC-9) cells after spontaneous cell fusion of drug-resistant and sensitive lineages to Gefitnib, an EGFR inhibitor. We demonstrate the presence of cell-cell fusion with nuclear fusion through several mechanisms, including fluorescent imaging, fluorescent activated cell sorting (FACS) analysis, and quantification of DNA content and cell-cycle analysis. We then examine the potential of fused NSCLC cells to propagate chemoresistance across different types and classes of NSCLC treatment. In addition, we analyze the genomic features that arise after fusion in NSCLC that could contribute to the promotion of cancer malignancy in NSCLC. We conclude that cell-cell fusion can serve to directly propagate and promote chemoresistance in NSCLC and that further study is needed to identify the full extent of the impact of cell-cell fusion on tumor evolution leading to treatment failure.

Results

Identification and Isolation of Cell-Cell Fusion in NSCLC

We identified cell-cell fusion in non-small cell lung cancer (NSCLC) during a long-term co-culture experiment designed to study the dynamics between drug-sensitive (parental) and drug-resistant (resistant) NSCLC cell populations. Parental and resistant cells were tagged with nuclear-localizing GFP and mCherry, respectively, and co-cultured at various initial ratios under control and gefitinib treatment conditions (20nM) for 12 weeks. Under control conditions, parental cells exhibited higher intrinsic fitness, resulting in an increased frequency, while resistant cells showed fitness costs and declined in frequency. In contrast, under gefitinib treatment, resistant cells gained a fitness advantage and predominated within the co-culture (**Figure 1A, B**).

Remarkably, a third cell population, expressing both GFP and mCherry, serendipitously emerged under gefitinib treatment. These yellow-fluorescing cells, indicative of cell-cell fusion, exhibited enhanced fitness and underwent clonal expansion both in the presence of gefitinib and during a subsequent drug-free recovery period (treatment holiday) lasting six weeks. Fused cells were isolated via fluorescence-activated cell sorting (FACS) for further characterization.

Importantly, our quantitative analysis revealed that the fused cell population constituted over 40% of the total cells in co-cultures initiated with a 1:1 parental-to-resistant cell ratio. Fusion rates were lower but still substantial in co-cultures with a 75:25 parental-to-resistant ratio (**Figure 1C**).

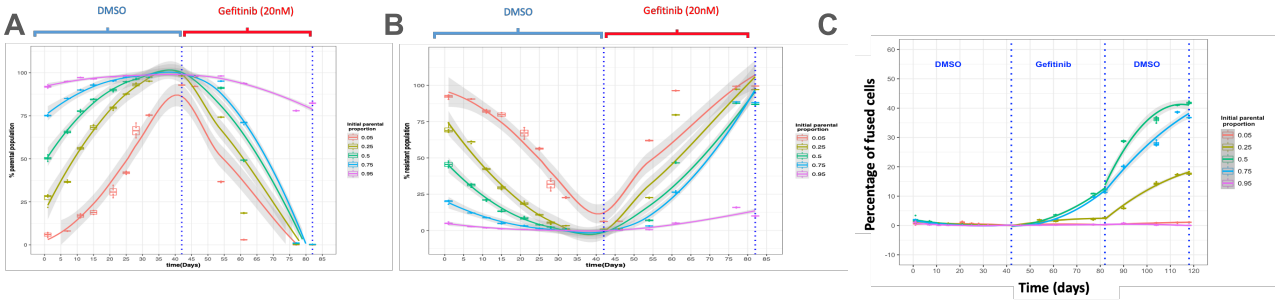

Figure 1. Repeated co-culture of chemosensitive (parental) and chemoresistant cells at different ratios yielded different proportions of fused cells. *A:* In the absence of drug, the parental cell population reached 80-100% confluence across all co-culture ratios before dropping steadily under Gefitinib selection. *B:* Chemoresistant cells approach extinction in the absence of drug across co-culture ratios, and clonally expand rapidly following administration of Gefitinib. *C:* Fused cells occurred spontaneously at low (1-2%) rates prior to Gefitinib selection. Following prolonged selection, fused cells reach varying levels of confluence 1-41% under different conditions. Co-culture of chemosensitive and chemoresistant cells in a 50-50 split yielded the highest percentage of fused cells.

To monitor the frequencies of parental and resistant cell populations and detect fusion events, we employed high-parameter flow cytometry, which provides detailed insights into heterogeneous cell populations with high sensitivity. Flow cytometry analysis revealed a distinct double-positive population expressing both GFP and mCherry, confirming the presence of cell-cell fusion (**Figure 2**).

Given that the fluorescent markers were nuclear-localizing, we hypothesized that these double-positive cells arose from nuclear fusion between the parental and resistant cells. This finding underscores the capacity of cell-cell fusion to generate genetically heterogeneous populations, potentially contributing to the evolution of cancer cells and the development of drug resistance in NSCLC cells under therapeutic pressure.

Following the isolation of the three cell populations - parental (chemosensitive), resistant, and fused – we performed additional characterization and confirmation studies.

To confirm that the observed fusion events involved nuclear fusion, we performed DAPI staining and fluorescence imaging to assess the co-localization of GFP and mCherry signals. The analysis revealed complete co-localization of GFP and mCherry fluorescence, appearing yellow when overlaid. Importantly, the co-localized GFP and mCherry signals were confined to the DAPI-stained nuclei, confirming that the fused cells indeed exhibited nuclear fusion (**Figure ??E**). These findings provide definitive evidence that the cell-cell fusion events observed in NSCLC co-cultures involve the integration of nuclei from parental and resistant cell populations, further highlighting the significance of this phenomenon under drug selection pressure.

To further ensure that the fused cells had undergone genetic mixing, we performed a cell-cycle analysis. In this experiment, we observed higher levels of DNA content in the fused cells across all phases of the cell cycle compared to either the parental

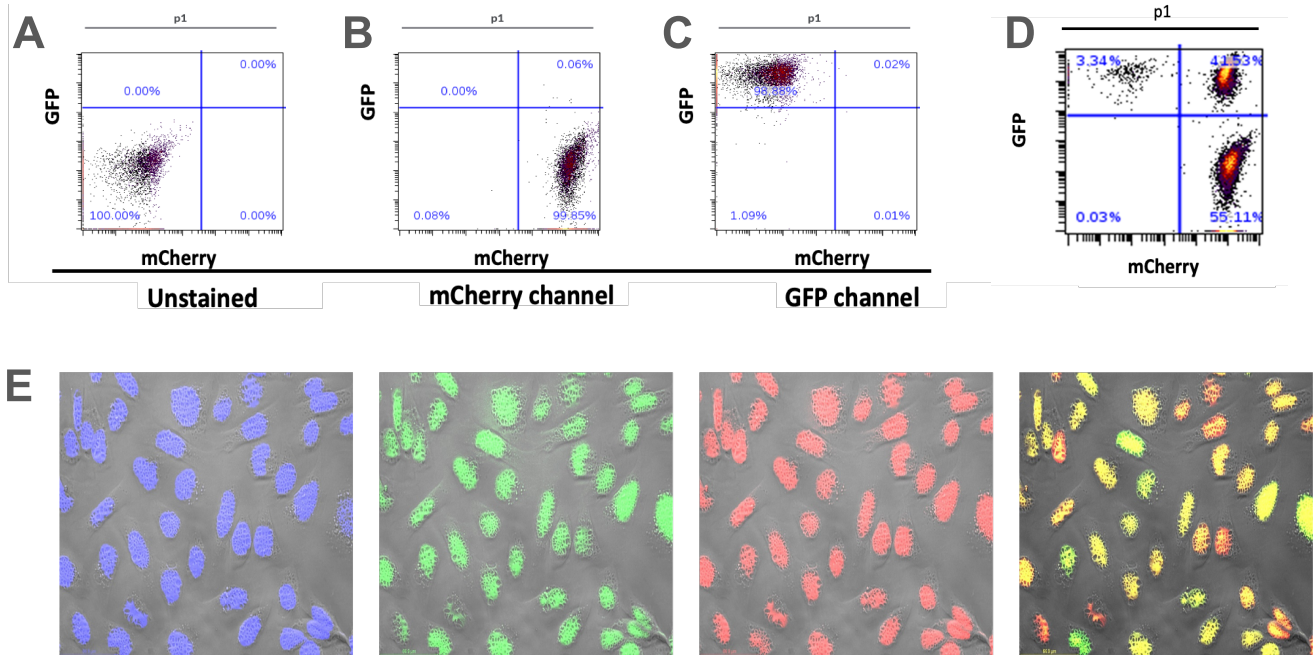

Figure 2. Fluorescent-activated cell sorting (FACS) confirms cell-cell fusion with nuclear fusion following 50-50 co-culture experiments. A: Untagged PC-9 cells served as a control, and demonstrated the absence of both GFP or mCherry signals at baseline. **B:** mCherry expression in isolated tagged resistant cell was observed in 99.85% of the cell population, confirming successful mCherry uptake. **C:** GFP expression in isolated tagged sensitive cells was observed in 99.88% of the cell population, confirming successful GFP uptake. **D:** Following long-term co-culture experiments with Gefitinib selection, identification of over 41% fused cells was confirmed with 41.53% co-expression of GFP and mCherry signals following FACS. The remaining cells expressed either mCherry (55.11%) or GFP (3.34%) alone. **E:** Staining confirms presence of nuclear fusion following cell-cell fusion of parental and resistant PC-9 cells. From left to right: Left: DAPI staining isolates nuclei in fused cells. Left Middle: Parental cells were tagged with nuclear-localizing GFP; imaging confirms retention of GFP following fusion. Right Middle: Resistant PC-9 cells were tagged with nuclear-localizing mCherry; imaging confirms retention of mCherry following fusion. Right: Combined fluorescent images demonstrates presence of co-expression of mCherry and GFP in fused nuclei following cell-cell fusion.

or resistant cells alone. These results are presented in **Figure 3.** The DNA content in fused cells is not exactly doubled however, and this likely reflects the many potential pathways cells can take following cell-cell fusion to maintain or reduce their ploidy.[2–4,8]

Evidence of Conferred Fitness Advantages Secondary to Cell-Cell Fusion

Following our isolation of fused cells, we evaluated the role of cell-cell fusion in contributing to cancer malignant potential through two mechanisms: propagation of chemoresistance and promotion of genetic heterogeneity.

Propagation of Chemoresistance

To characterize the effect of cell-cell fusion on chemoresistance in NSCLC cells, we performed a series of cell viability assays comparing the survival of our parental, resistant (to Gefitinib), and fused cell lines in the presence of 12 different chemotherapeutics. The selection of chemotherapeutics spanned several different classes of chemotherapeutics currently used to treat NSCLC, including EGFR inhibitors, Tyrosine Kinase Inhibitors (TKIs), DNA repair inhibitors, and taxanes.[9,10] In alphabetical order, the drugs we evaluated are: cisplatin, crizotinib, erlotinib, ganetesipib, gefitinib, gemcitabine, lapatinib, osimertinib, paclitaxel, pemextred, topotecan, and trametinib.

Across the 12 drugs we evaluated, the fused cells consistently matched or exceeded the cell viability levels of the chemoresistant cells, both of which consistently outperformed the chemosensitive parental cells. These results were consistent across all drug dosages, but in some cases the drug concentrations eventually hit sufficiently high concentrations where all three

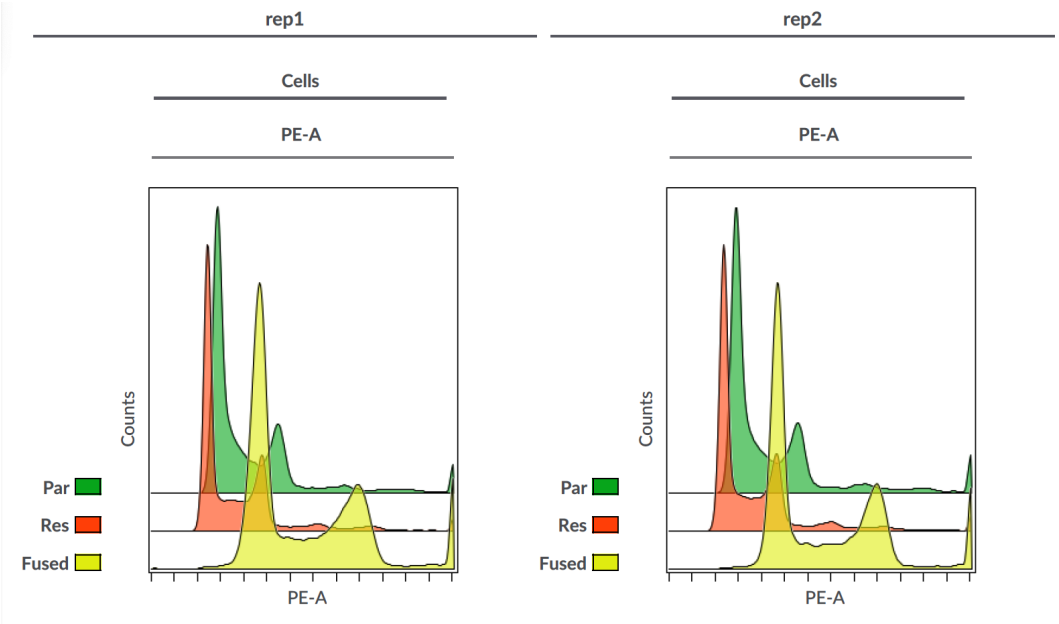

Figure 3. Cell-cycle analysis provides evidence of nuclear fusion by demonstrating higher DNA content of fused (Fused) cells relative to parental (Par) or resistant (Res) cells, across two experimental replicates. All three cell populations – parental, resistant, and fused – had similar cell counts in each phase of the cell cycle. The first spike represents G1, the lull in between the first and second spike represents S, and the second spike represents G2. The overall right-shift of the curve of the fused cells confirms higher than average levels of DNA content in each phsed compared to the other two cell populations.

cell populations lost cell viability. The individual drug response curves for these 12 experiments can be seen in **Figure 6**. For ease of interpretability, our cell viability assay results at the maximum evaluated dosages are further summarized in **Figure 4**.

BulkRNAseq and Evidence of the Potentiation of Cancer Hallmarks

Previous studies have shown that spontaneous cell-cell fusion with nuclear fusion leads to increased genome instability and can potentiate tumor evolution in breast cancer.[4] As another epithelial based cancer, we anticipated that NSCLC would have similar characteristics, especially following our observations of nuclear fusion. To evaluate the role of fusion in potentiating cancer hallmarks in NSCLC, we conducted differential gene expression and gene set enrichment analyses across our three cell lines of interest (parental, resistant, and fused).

Given the similarity in drug profiling between the fused and resistant cell lines, we anticipated that the fused cells would more closely imitate their chemoresistant lineage compared to their parental lineage. However, as reflected in **Figure 5**, the differential gene analysis found that different samples of fused cells had expression profiles similar to both the parental and resistant cell lines.

Despite their shared genomic patterns, the fused cells appeared to have distinct genomic features compared to either of their cell lineages. Gene set enrichment analysis revealed that the most differentially expressed genes in fused cells were cenrtalized across several key processes including cell cycle regulation and epithelial mesenchymal transition (EMT). The top 5 gene set enrichment analysis results are summarized in descending order of statistical significance in **Table 1.** Both EMT and uncontrolled cellular growth (due to dysregulated cell cycle control) are cancer hallmarks, and thus our prelimiary analysis provides further evidence that cell-cell fusion can potentiate tumor malignant potential.

Discussion

Cell-cell fusion is a complex process that occurs throughout the human physiology and pathology.[2] There has been increasing evidence that cell-cell fusion contributes to tumor malignancy through a variety of mechanisms related to the cancer hallmarks, from promoting cancer stemness and proliferative potential[11–14] to enabling the epithelial-mesenchymal transition and metastasis.[14–16] Despite these recent research advances, the process of cell-cell fusion has not been studied extensively in many cancers, including non-small cell lung cancer (NSCLC).[2,4]

Prior studies have primarily investigated the role of cancer cell-somatic cell fusion in other epithelial cancers, with observed effects ranging from potentiating immune evasion[8,17–19] and local invasion of surrounding tissues. Only recently have studies

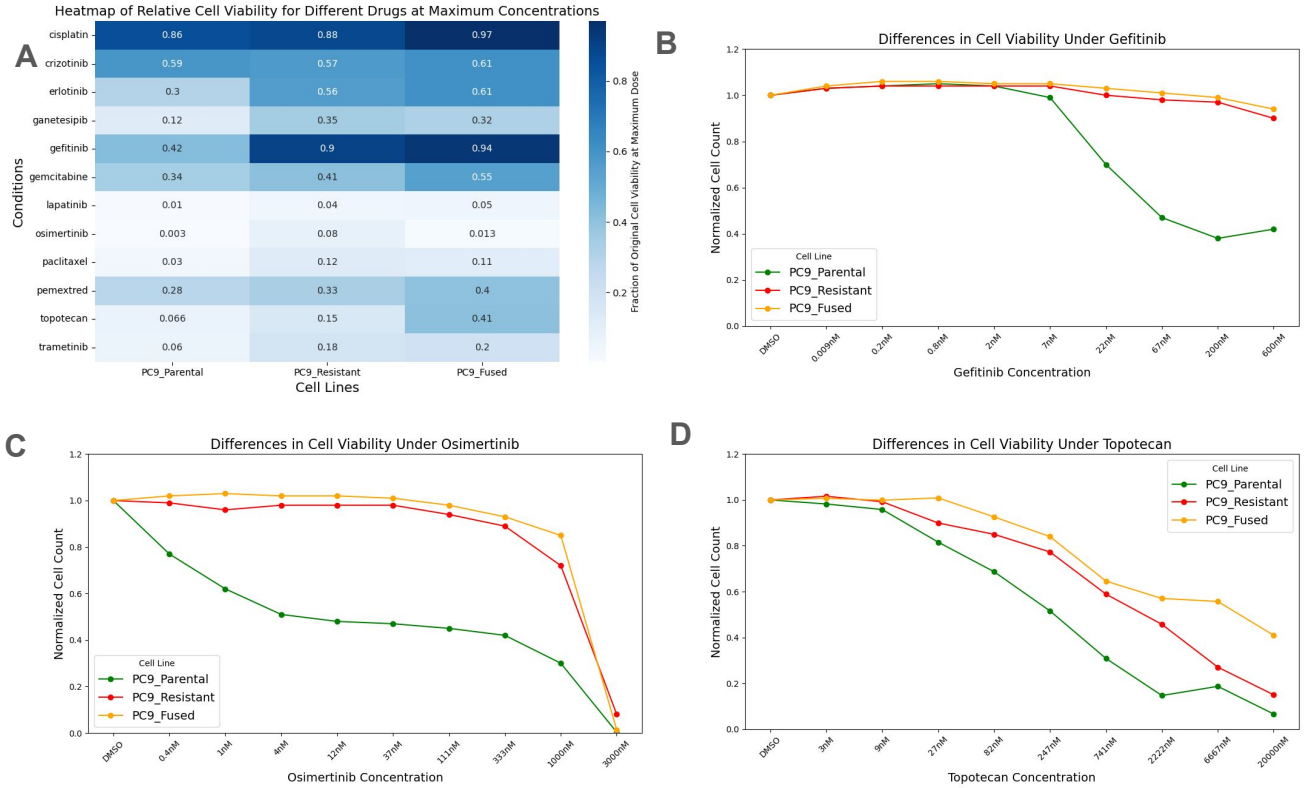

Figure 4. Cell viability assay results demonstrate that the Fused PC-9 cells consistently demonstrate conserved inheritance of chemoresistance under maximum drug dose conditions across 12 different chemotherapeutics. A: While the fused cells can match the survivability of their resistant cell lineage (as in the case of savolitinib and paclitaxel), there are several cases where the fused cells demonstrate even higher rates of collateral resistance compared to either of their lineages of origin. **B-D:** Illustrative examples of the drug response curves of parental, fused, and resistant cells under osimertinib(B), gefitinib(C) and topotecan(D). Full panel of results for all 12 drugs can be found in Supplemental Figure 1.

expanded their purview to consider intratumor cell-cell fusion and its potential to accelerate tumor evolution and rates of treatment failure.[4,20–22]

In this study, we isolated and characterized cells derived from the cell-cell fusion of two different NSCLC cell lineages. Over the course of a prolonged coculture experiment between our GFP-parental and mCherry-resistant NSCLC cell lines, we observed that cell-cell fusion occurred at low constant rates (1-2%) in the absence of drug. However, once chemotherapeutics were applied, this selective pressure favored cells with chemoresistant drug profiles including our original resistant cells and their fused counterparts. Furthermore, when collateral drug sensitivities were evaluated using cell viability assays, we found that the propagation of chemoresistance extended beyond the drug that the cells had originally evolved resistance to. In fact, the improved cell viability of fused cells in high doses of chemotherapy was consistent across 12 different drugs used today in the control of NSCLC, across several different chemotherapeutic classes and mechanisms of actions.

Importantly, this demonstrates a key insight into the potential clinical impacts of cell-cell fusion. While cell-cell fusion is a fundamentally rare event, the adaptive benefits it can provide seem to be selected for in tumor environments, particularly once treatments are administered. This idea is not completely novel; this approach to oncological research where tumor dynamics are evaluated through an evolutionary lens is known as evolutionary oncology.[23–26] However, this perspective supports the further evaluation of cell-cell fusion as a future chemotherapeutic target; rare events can still have tremendous clinical impacts.

Following the identification and confirmation of our nuclear fusion in our fused cells, we were interested in looking at the genomic profile of the fused cells as it related to their cellular origins (our parental and Gefitinib resistant PC-9 cells). Our preliminary bulkRNAseq analyses provides further evidence that intratumor cell-cell fusion can potentiate cancer hallmarks similarly to more classic examples of heterotypic cell fusion in cancer. While our genomic characterization of fused cells is in its early stages, it offers important insight into the importance of increased study into cell-cell fusion across cancer types.

Our recent review paper suggests that cell-cell fusion could become the next cancer hallmark in its own right, but that there is insufficient evidence for its occurrence and importance across cancer subtypes for this to be established at present.[2] This study

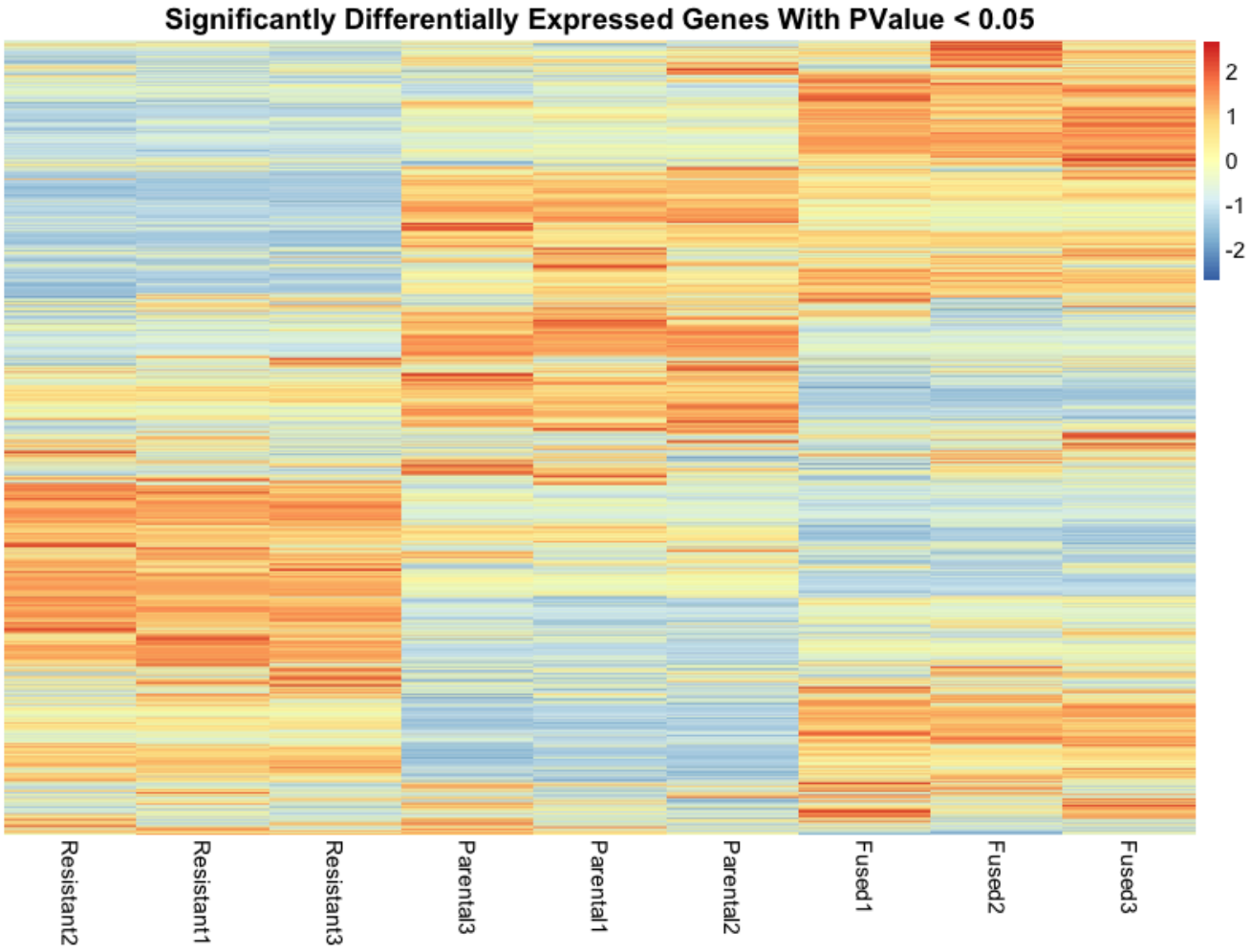

Figure 5. BulkRNAseq analysis reveals genomic heterogeneity following cell-cell fusion.

supports this claim by providing important initial identification and characterization of cell-cell fusion in NSCLC, one of the deadliest cancers at present, and demonstrating its potential clinical impacts. Overall, we conclude that cell-cell fusion requires further study to more directly elucidate its mechanisms of impact on tumor evolution and the rise in treatment failure. This study is an important first step towards elucidating the roles and mechanisms of cell-cell fusion in cancer. We anticipate that with further study, cell-cell fusion will offer a new avenue forward towards novel chemotherapeutics and improved treatment outcomes for cancer patients everywhere.

Methods

Cell lines

Ancestral NSCLC PC-9 cells (Sigma-Aldrich, 90071810) were cultured in RPMI-1640 medium supplemented with 10% heat-inactivated fetal bovine serum and 1% penicillin/streptomycin. To create distinct drug-sensitive and drug-resistant populations, cells were labeled with eGFP and mCherry fluorescent proteins, respectively. Drug-sensitive cells were maintained in 0.1% DMSO as a vehicle control, while resistant cells were cultured in 1 μM gefitinib (Cayman, 13166) following protocols described by Farrokhian et al.[27].

Derivation of Fused Cells Using Co-culture experiments

To assess the long-term dynamics of cell-cell interactions and fitness across untreated and treated conditions, we co-cultured drug-sensitive and drug-resistant cell populations at five distinct ratios. Briefly, a total of 1×10^5 cells, comprising both populations in varying proportions, were seeded into a 10cm² tissue culture-treated dish and maintained in 0.1% DMSO as vehicle control for an initial period of six weeks. When cultures reached 80–90% confluence, cells were subcultured into fresh

Table 1. Gene Set Enrichment Analysis (GSEA) Reveals Novel Patterns of Expression Post-Fusion Compared to Resistant and Sensitive Cell Lineages.

ID	Description	setSize	enrichmentScore	NES	p.adjust
HALLMARK_E2F_TARGETS	Genes encoding cell cycle related targets of E2F transcription factors.	200	-0.635	-2.515	0.00e+00
HALLMARK_MYC_TARGETS_V1	A subgroup of genes regulated by MYC - version 1 (v1).	200	-0.607	-2.405	0.00e+00
HALLMARK_G2M_CHECKPOINT	Genes involved in the G2/M checkpoint, as in progression through the cell division cycle.	199	-0.555	-2.199	0.00e+00
HALLMARK_EPITHELIAL_MESENCHYMAL_TRANSITION	Genes defining epithelial-mesenchymal transition, as in wound healing, fibrosis and metastasis.	165	-0.549	-2.132	2.00e-07
HALLMARK_MYC_TARGETS_V2	A subgroup of genes regulated by MYC - version 2 (v2).	58	-0.704	-2.329	2.20e-06
HALLMARK_SPERMATOGENESIS	Genes up-regulated during production of male gametes (sperm), as in spermatogenesis.	82	-0.471	-1.658	3.01e-02
HALLMARK_KRAS_SIGNALING_UP	Genes up-regulated by KRAS activation.	146	-0.397	-1.518	3.30e-02
HALLMARK_IL2_STAT5_SIGNALING	Genes up-regulated by STAT5 in response to IL2 stimulation.	166	-0.335	-1.301	2.40e-01
HALLMARK_ESTROGEN_RESPONSE_LATE	Genes defining late response to estrogen.	177	-0.317	-1.238	3.44e-01
HALLMARK_ALLOGRAFT_REJECTION	Genes up-regulated during transplant rejection.	133	-0.340	-1.280	3.84e-01

medium, and samples were collected at each subculturing interval to monitor population frequencies. These frequencies were analyzed using high-parameter, high-sensitivity flow cytometry (Sony ID70000). Following the initial six weeks, co-cultured populations were exposed to 20nM gefitinib and cultured under these conditions for an additional six weeks, with population frequencies similarly analyzed at each subculturing interval to assess proportions under drug selection pressure. After 12 weeks of co-culturing, double-positive cell populations that emerged were sorted and maintained in a medium containing 20nM gefitinib to study the stability and characteristics.

Nuclear staining

To investigate nuclear fusion events in fused NSCLC cell populations compared to parental cell populations, we performed DAPI staining using 8-well chambered µ-slides (ibidi, 80806) followed by fluorescence microscopy. Cells were seeded at a density of 5×10^4 per well. Once cells adhered to the slide, the medium was removed, and cells were fixed with 4% formaldehyde (prepared in 1X PBS) for 10 minutes at room temperature to preserve cellular structures. After fixation, formaldehyde was discarded, and samples were washed three times with 1X PBS. Cells were then permeabilized with a solution of 0.1% Triton X-100 in 1X PBS for 15 minutes at room temperature. Following permeabilization, the solution was removed, and a drop mounting media containing DAPI (Abcam, ab104139) was added to each well. Coverslips were carefully placed over the cells, and fluorescence images were captured using Leica fluorescence microscope to visualize nuclear fusion.

Cell Cycle Analysis

To assess cell cycle distribution, we utilized propidium iodide (PI) staining to quantify DNA content. Experimentally, cells were harvested and thoroughly washed with PBS to eliminate residual medium and drug. After washing, cells were fixed in cold 70% ethanol at 4°C for 30 minutes, then washed twice in PBS to remove the remaining ethanol. Samples were subsequently stained with FxCycle PI/RNase staining solution (Molecular Probes, F10797) following the manufacturer's protocol. Stained samples were analyzed using flow cytometry, allowing for detailed determination of cell cycle distribution based on DNA content.

Drug sensitivity profiling

To assess drug sensitivity, cells were harvested at 70–80% confluence and counted using 0.4% trypan blue solution (Thermo Fisher, 15250061) with Countess 3 Automated Cell Counter (Life Technologies). For cell viability assays, 3,000 cells per well in 100 µL of medium containing increasing concentrations of selected drugs were plated in 96-well microplates (Corning, 3904) in triplicate for drug-sensitive, drug-resistant, and fused cell populations. Plating was performed using a Multidrop reagent dispenser (Thermo Fisher) to ensure consistency. Drug-treated cells were incubated for 3 days, after which cell viability was measured using the CellTiter-Glo luminescent assay (Promega, G7571), with a luminescence signal read on a Tecan microplate reader. The resulting cell viability data were normalized to the average of DMSO-treated control and plotted as relative dose-response curves across the different cell types.

Bulk RNAseq: Library Preparation, Quality Control, and Sequencing

Total RNA was extracted in triplicate from drug-sensitive PC-9, drug-resistant PC-9, and fused cell populations cultured as described above, using the Trizol RNA isolation reagent following the manufacturer's instructions (Thermo Fisher Scientific, 15596026). RNA quality and integrity were evaluated using a NanoDrop spectrophotometer and Agilent TapeStation systems, while RNA concentration was determined using the Qubit RNA Broad Range (BR) assay kit (Thermo Fisher, Q10210). For library preparation, 500 ng of total RNA was used as input for the Illumina TruSeq RNA Library Prep Kit v2 (Illumina), following Illumina's recommended protocol. The final libraries underwent quality assessment using TapeStation systems (Agilent) and quantification by Qubit (Thermo Fisher). Finally, sequencing was performed on the Illumina NovaSeq SP platform with 150 bp paired-end reads (2×150 bp).

Bulk RNAseq: Sequence Alignment and Analyses

Read alignment and quantification is done via the STAR/Salmon workflow. We first filtered and adapter trimmed the paired-end reads using fastp with default settings. Subsequently the trimmed reads are aligned to GRCh38 primary assembly with gencode gene annotations v42 via STAR with two-pass mode and chimeric read detection enabled. Following the alignment, reads mapping to the transcript locations are quantified via Salmon with bootstrapping enabled. Transcript level quantifications (TPMs) are then used to calculate gene-level counts using the tximport package. Calculated gene-level counts are then used as input to edgeR based differential expression analysis workflow.

Following the transcript-level alignment, gene-level counts were generated using the tximport package[28]. Differential gene expression was run using the edgeR package[29]. Gene set enrichment (GSEA) and gene ontology enrichment analyses were performed using the clusterProfiler package.[30] Plotting used a combination of ggplot2 and pheatmap.[31,32]

References

1. Hernández, J. M. & Podbilewicz, B. The hallmarks of cell-cell fusion, DOI: 10.1242/dev.155523 (2017). ISSN: 14779129 Issue: 24 Pages: 4481-4495 Publication Title: Development (Cambridge) Volume: 144.
2. Shultes, P. V., Weaver, D. T., Tadele, D. S., Barker-Clarke, R. J. & Scott, J. G. Cell-cell fusion in cancer: The next cancer hallmark? *The Int. J. Biochem. Cell Biol.* **175**, 106649, DOI: https://doi.org/10.1016/j.biocel.2024.106649 (2024).
3. Brukman, N. G., Uygur, B., Podbilewicz, B. & Chernomordik, L. V. How cells fuse, DOI: 10.1083/jcb.201901017 (2019). ISSN: 15408140 Issue: 5 Pages: 1436-1451 Publication Title: Journal of Cell Biology Volume: 218.
4. Miroshnychenko, D. *et al.* Spontaneous cell fusions as a mechanism of parasexual recombination in tumour cell populations. *Nat. Ecol. Evol.* **5**, 379–391, DOI: 10.1038/s41559-020-01367-y (2021). Publisher: Nature Research.
5. Hendriks, L. E. L. *et al.* Non-small-cell lung cancer. *Nat. Rev. Dis. Primers* **10**, 71, DOI: 10.1038/s41572-024-00551-9 (2024).
6. Yeldag, G., Rice, A. & del Río Hernández, A. Chemoresistance and the Self-Maintaining Tumor Microenvironment. *Cancers* **10**, 471, DOI: 10.3390/cancers10120471 (2018).
7. Tajima, Y., Shibasaki, F. & Masai, H. Cell fusion upregulates PD-L1 expression for evasion from immunosurveillance. *Cancer Gene Ther.* **31**, 158–173, DOI: 10.1038/s41417-023-00693-0 (2024).
8. Hass, R., Ohe, J. v. d. & Dittmar, T. Hybrid formation and fusion of cancer cells in vitro and in vivo, DOI: 10.3390/cancers13174496 (2021). ISSN: 20726694 Issue: 17 Publication Title: Cancers Volume: 13.
9. Alduais, Y., Zhang, H., Fan, F., Chen, J. & Chen, B. Non-small cell lung cancer (NSCLC): A review of risk factors, diagnosis, and treatment. *Medicine* **102** (2023).
10. Guo, Q. *et al.* Current treatments for non-small cell lung cancer. *Front. Oncol.* **12**, DOI: 10.3389/fonc.2022.945102 (2022).
11. Zhang, S. *et al.* Generation of Cancer Stem-like Cells through Formation of Polyploid Giant Cancer Cells. *Oncogene* **33**, 10.1038/onc.2013.96, DOI: 10.1038/onc.2013.96 (2014).
12. Uygur, B. *et al.* Interactions with muscle cells boost fusion, stemness, and drug resistance of prostate cancer cells. *Mol. Cancer Res.* **17**, 806–820, DOI: 10.1158/1541-7786.MCR-18-0500 (2019). Publisher: American Association for Cancer Research Inc.
13. Dittmar, T. Generation of Cancer Stem/Initiating Cells by Cell–Cell Fusion, DOI: 10.3390/ijms23094514 (2022). ISSN: 14220067 Issue: 9 Publication Title: International Journal of Molecular Sciences Volume: 23.
14. Melzer, C., Ohe, J. v. d. & Hass, R. In Vitro Fusion of Normal and Neoplastic Breast Epithelial Cells with Human Mesenchymal Stroma/Stem Cells Partially Involves Tumor Necrosis Factor Receptor Signaling. *Stem Cells* **36**, 977–989, DOI: 10.1002/stem.2819 (2018). Publisher: Wiley-Blackwell.
15. Hass, R., von der Ohe, J. & Dittmar, T. Cancer Cell Fusion and Post-Hybrid Selection Process (PHSP). *Cancers* **13**, 4636, DOI: 10.3390/cancers13184636 (2021). Number: 18 Publisher: Multidisciplinary Digital Publishing Institute.
16. Dietz, M. S. *et al.* Relevance of circulating hybrid cells as a non-invasive biomarker for myriad solid tumors. *Sci. Reports* **11**, 1–13, DOI: 10.1038/s41598-021-93053-7 (2021). Number: 1 Publisher: Nature Publishing Group.
17. Bateman, A., Bullough, F. & Murphy, S. Fusogenic Membrane Glycoproteins As a Novel Class of Genes for the Local and Immune-mediated Control of Tumor Growth 1 (2000). Pages: 1492-1497 Publication Title: CANCER RESEARCH Volume: 60.
18. Tretyakova, M. S., Subbalakshmi, A. R., Menyailo, M. E., Jolly, M. K. & Denisov, E. V. Tumor Hybrid Cells: Nature and Biological Significance. *Front. Cell Dev. Biol.* **10** (2022).

19. Shin, J. H. *et al.* Colon cancer cells acquire immune regulatory molecules from tumor-infiltrating lymphocytes by trogocytosis. *Proc. Natl. Acad. Sci.* **118**, e2110241118, DOI: 10.1073/pnas.2110241118 (2021). Publisher: Proceedings of the National Academy of Sciences.

20. Bühler, A. *et al.* When Mechanical Stress Matters: Generation of Polyploid Giant Cancer Cells in Tumor-like Microcapsules, DOI: 10.1101/2022.09.22.508846 (2022). Pages: 2022.09.22.508846 Section: New Results.

21. Demin, S., Berdieva, M. & Goodkov, A. Cell-cell fusions and cell-in-cell phenomena in healthy cells and cancer: Lessons from protists and invertebrates. *Semin. Cancer Biol.* **81**, 96–105, DOI: 10.1016/j.semcancer.2021.03.005 (2022).

22. Dittmar, T., Weiler, J., Luo, T. & Hass, R. Cell-Cell Fusion Mediated by Viruses and HERV-Derived Fusogens in Cancer Initiation and Progression. *Cancers* **13**, 5363, DOI: 10.3390/cancers13215363 (2021). Number: 21 Publisher: Multidisciplinary Digital Publishing Institute.

23. Cairns, J. Mutation selection and the natural history of cancer. *Nature* **255**, 197–200, DOI: 10.1038/255197a0 (1975).

24. Scarborough, J. A., Eschrich, S. A., Torres-Roca, J., Dhawan, A. & Scott, J. G. Exploiting convergent phenotypes to derive a pan-cancer cisplatin response gene expression signature. *NPJ Precis. Oncol.* **7**, 38 (2023).

25. Maltas, J. *et al.* Frequency-dependent ecological interactions increase the prevalence, and shape the distribution, of preexisting drug resistance. *PRX Life* **2**, 023010, DOI: 10.1103/PRXLife.2.023010 (2024).

26. King, E. S., Tadele, D. S., Pierce, B., Hinczewski, M. & Scott, J. G. Diverse mutant selection windows shape spatial heterogeneity in evolving populations. *PLOS Comput. Biol.* **20**, 1–22, DOI: 10.1371/journal.pcbi.1011878 (2024).

27. Farrokhian, N. *et al.* Measuring competitive exclusion in non–small cell lung cancer. *Sci. Adv.* **8**, eabm7212 (2022).

28. Soneson, C., Love, M. I. & Robinson, M. D. Differential analyses for rna-seq: transcript-level estimates improve gene-level inferences. *F1000Research* **4**, DOI: 10.12688/f1000research.7563.1 (2015).

29. Robinson, M. D., McCarthy, D. J. & Smyth, G. K. edger: a bioconductor package for differential expression analysis of digital gene expression data. *Bioinformatics* **26**, 139–140, DOI: 10.1093/bioinformatics/btp616 (2010).

30. Yu, G., Wang, L.-G., Han, Y. & He, Q.-Y. clusterprofiler: an r package for comparing biological themes among gene clusters. *OMICS: A J. Integr. Biol.* **16**, 284–287, DOI: 10.1089/omi.2011.0118 (2012).

31. Wickham, H. *ggplot2: Elegant Graphics for Data Analysis* (Springer-Verlag New York, 2016).

32. Kolde, R. *pheatmap: Pretty Heatmaps* (2019). R package version 1.0.12.

Acknowledgements

JGS and PVS were supported by NIH 5R37CA244613-04 (https://www.cancer.gov/). PVS was supported by NIH 3T32GM007250-46S1 (https://www.nigms.nih.gov/). JGS was supported by American Cancer Society Research Scholar Grant RSG-20-096-01 (https://www.cancer.org/). DST was supported by The Research Council of Norway with grant 325628/IAR (https://www.forskningsradet.no/en/
The funders had no role in study design, data collection and analysis, decision to publish, or preparation of the manuscript.

Author contributions statement

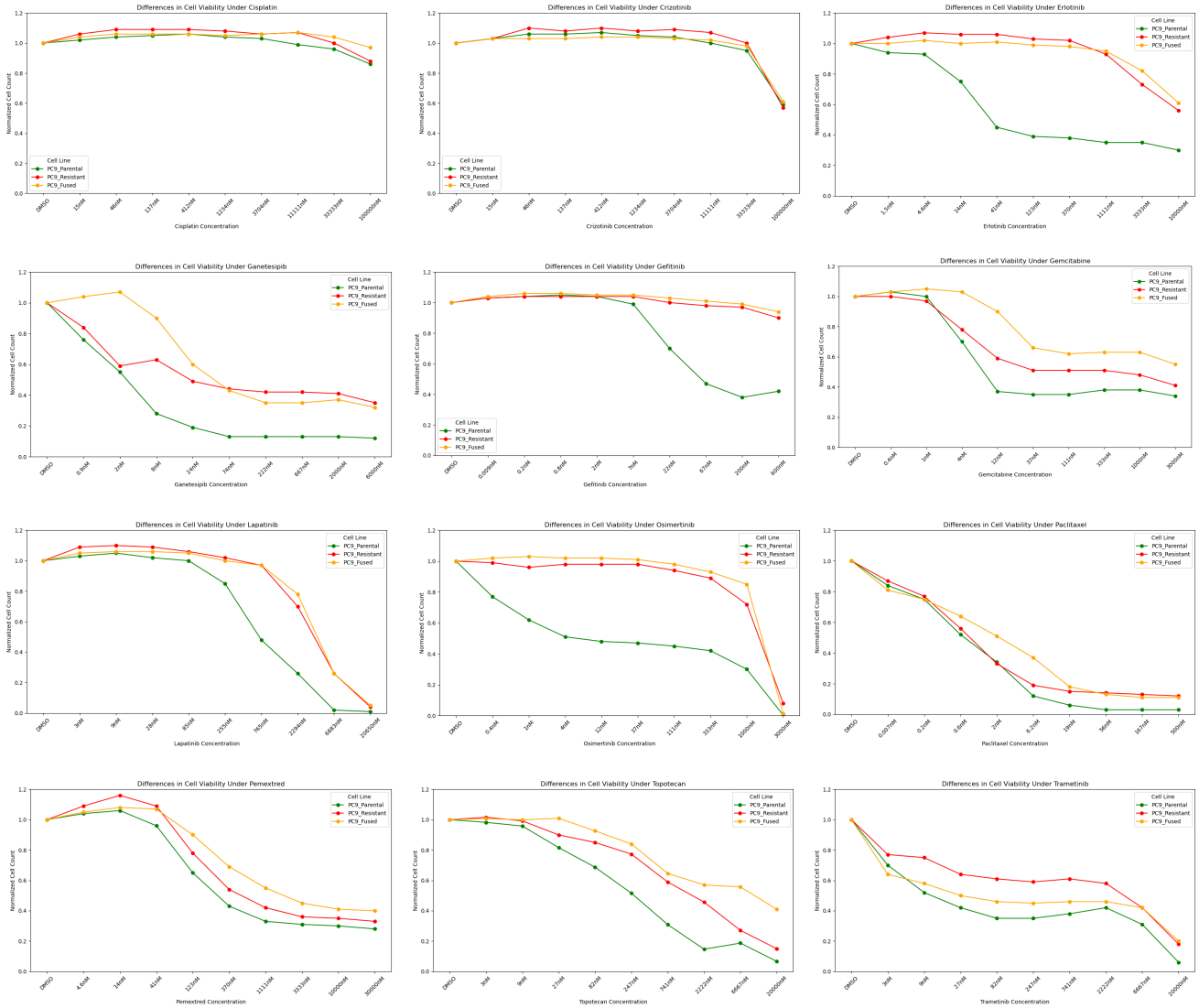

Figure 6. Supplemental Figure 1: Individual cell viability assays demonstrate consistent propagation of chemoresistance from resistant to fused cell lines. We individually administered 12 different chemotherapeutics to our three lineages of PC-9 cells and found that fused cells consistently had higher survivability relative to both the original parent cell-lines and the cell line with evolved resistance to Gefitinib. The drugs are listed alphabetically, reading the panel from left to right and inlcude: cisplatin, crizotinib, erlotinib, ganetesipib, gefitinib, gemcitabine, lapatinib, osimertinib, paclitaxel, pemextred, topotecan, and trametinib.